Formation of mesoporous SBA-15 from a colloidal perspective

Linton, Peter

2009

[Link to publication](#)

Formation of mesoporous SBA-15 from a colloidal perspective

Peter Linton

Formation of mesoporous SBA-15 from a colloidal perspective

Peter Linton

Physical Chemistry

LUND UNIVERSITY

3

Populärvetenskaplig sammanfattning

Syftet med denna avhandling är att, från fysikalkemisk synvinkel, försöka förstå hur och varför mesoporösa material bildas. Istället för att arbeta i blindo kan den ökade förståelsen användas till att kontrollera och optimera de tillverkade materialen. Mesoporösa material är extremt porösa och dess väggar består av kiseldioxid. På grund av porositeten så har materialen en väldigt stor ytarea. 7g av materialet kan ha en ytarea stor som en fotbollsplan. Porositeten, den stora ytarean samt den stabila strukturen gör materialet väldigt intressant ur applikationsyfte och industriell verksamhet. Det bedrivs mycket forskning på hur materialen kan användas inom katalys och för separationsprocesser, men det finns även förhoppningar att de skall kunna användas som bärare av aktiva substanser, inom optik och dielektriska material etc. Än så länge har materialen inte fått sitt stora genombrott på marknaden.
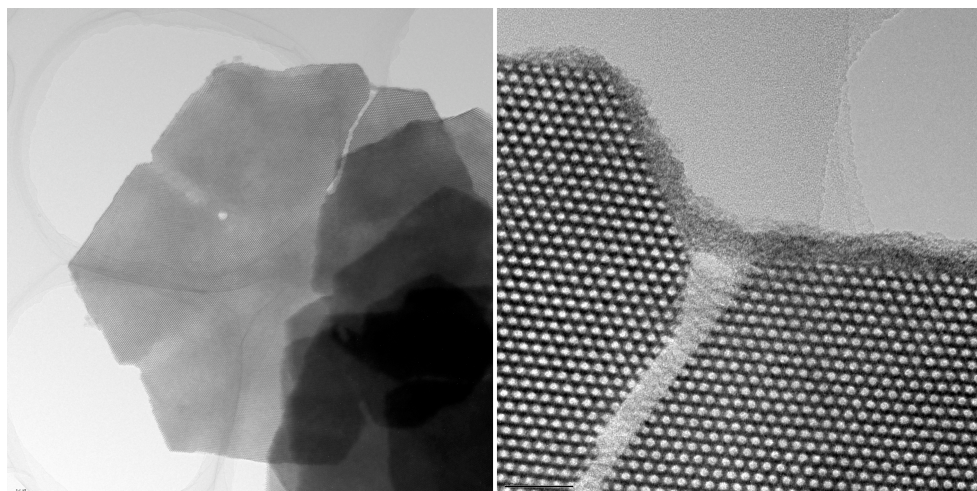
Figur 1. Elektronmikroskopibilder av mesoporöst materal. Bilden till vänster visar hur en partikel kan se ut, medan bilden till höger visar porerna i partikeln. Scale bar: 200nm (till vänster) och 50nm (till höger)

Denna avhandling fokuserar inte, direkt, på tillämpningar av materialen. Istället har mycket av arbetet varit koncentrerat på syntesen och dess olika komponenter. Det är ganska lätt att syntesisera mesoporösa material, däremot är processerna som styr

bildandet komplexa. Arbetet innefattar en större kunskap om yt- och kolloidkemi, en inriktning inom den fysikaliska kemin. Syntesen går till på följande sätt, en amfifilisk polymer och en kiseldioxid blandas i vatten med mycket lågt pH (Figur 2). Polymeren och kiselkällan interagerar, vilket resulterar i det mesoporösa materialet. En polymer är en molekyl som består av repeterande enheter av mindre molekyler (monomer). Om polymeren består av en del som tycker om vatten (hydrofil) och en del som inte tycker om vatten (hydrofob), så kommer den bilda, oftast, sfäriska aggregat i vatten. Den hydrofila delen kommer sträckas ut för att maximera kontakten med vatten, medan den hydrofoba delen kommer försöka minimera kontakten med vatten och istället föredra den inre delen av aggregatet. Dessa aggregat utgör en mall och kommer i slutet av syntesen finnas i porerna. Kiseldioxiden lägger sig runt aggregaten varpå många sfäriska aggregat klumpar ihop till en större partikel. Inne i denna större partikel packar sig polymeraggregaten. Under hela den här processen polymeriseras kiselkällan, vilket i förlängningen betyder att det större aggregatet hålls ihop i denna större enhet. Porerna är fyllda med polymer och för att frigöra porerna bränns polymeren bort i en 500°C varm ugn. Kvar finns det mesoporösa kiseldioxid materialet.
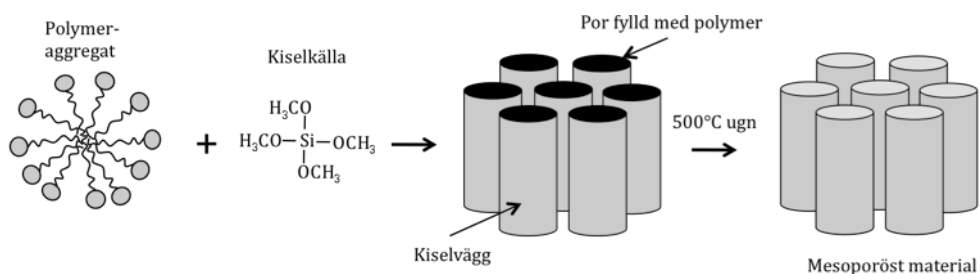
Figur 2. Schematisk bild av bildningen av mesoporöst kiseldioxid

Avhandlingen beskriver hur en viss typ av mesoporösa material bildas. De olika förloppen som styr syntesen har satts på en tidsaxel. I och med att information om när vissa steg startar och slutar, så går det att specifikt påverka dessa steg. Partikelstorleken kan varieras genom att t.ex. "störa" syntesen vid en viss tidpunkt under bildandet av materialet. Denna avhandlingen beskriver vikten av en bättre förståelse för hur materialen bildas och hur det kan användas för att styra och kontrollera materialen.

List of papers

I. **Growth and morphology of mesoporous SBA-15 particles**
    P. Linton and V. Alfredsson
    Chemistry of Materials, **2008**, *20* (9), 2878-2880

II. **In situ observation of the genesis of mesoporous silica SBA-15: dynamics on length scales from 1nm to 1μm**
    P. Linton, A. R. Rennie, M. Zackrisson and V. Alfredsson
    Langmuir, **2009**, *25* (8), 4685-4691

III. **The formation mechanism of mesoporous SBA-15 – an in situ small angle neutron scattering study**
    P. Linton, A. R. Rennie and V. Alfredsson
    Manuscript

IV. **The role played by salts in the kinetic of formation of SBA-15, an in-situ small angle X-ray diffraction study**
    C. V. Teixeira, H. Amenitsch, P. Linton, M. Linden and V. Alfredsson
    Manuscript

V. **Morphology of SBA-15 – directed by association processes and surface energies**
    P. Linton, J-C. Hernandez-Garrido, P. A. Midgley, H. Wennerström and V. Alfredsson
    Phys. Chem. Chem. Phys. **2009**, DOI:10.1039/b913755f

VI. **Controlling particle morphology and size in the synthesis of mesoporous SBA-15 materials**
    P. Linton, H. Wennerström and V. Alfredsson
    Submitted to PCCP

Contents

1. Introduction

Mesoporous materials have a structure that is atomically amorphous but mesoscopically ordered. The structures are analougues to those formed by lyotropic liquid crystals. The materials are formed in a cooperative self-assembly process with an inorganic source, frequently a silica source, and a structure promoter (an amphiphile). A number of methodologies can be used to produce these materials but the most frequently used and perhaps the most flexible one is to use a dilute solution of the amphiphile, a micellar solution, and to this add an inorganic source. The material will, with time, precipitate. The precipitate consists of an inorganic-amphiphilic composite and the porous material is generated when the amphiphile is removed.

The main objective of this thesis is to increase the understanding of the formation mechanism of mesoporous materials, with a focus on SBA-15*.[1] By in-situ methods the series of events that are essential for forming the material were investigated[2-4], a model based on surface energy arguments was developed[5] to explain the colloidal aspects (morphology and particle size) observed for a range of materials and also the particle size/morphology was controlled by specific intervention to an ongoing syntheses.[6, 7] Even though the structural and micellar evolution have been investigated the focus has been on the colloidal aspects of the formation.

Typically, synthesis of mesoporous materials is a straightforward procedure but the chemical and physical processes that drive the formation are complex. From results in previous studies as well as from the results presented in this thesis the formation steps in the synthesis of SBA-15 are summarized and depicted in figure 1.1.

---

* SBA-15 is the 2D hexagonal structure first synthesised by Zhao et. al. The structure promoter is a Pluronic polymer, an amphiphilic triblock coploymer.
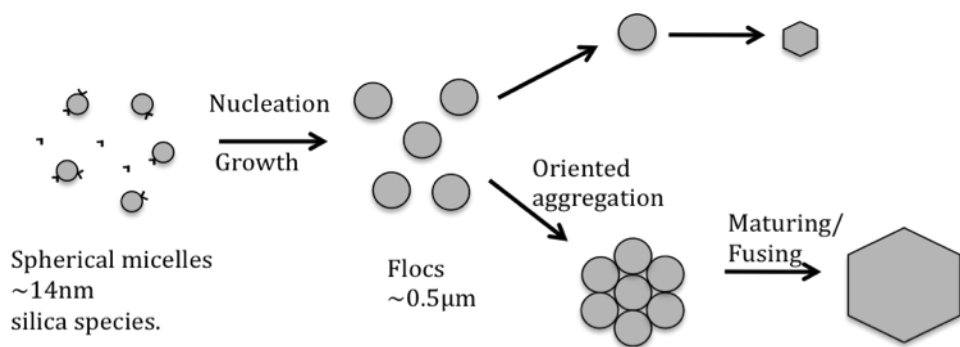
Figure 1.1. Schematic picture of the formation of mesoporous silica SBA-15. The steps are explained in the text.

The synthesis is initiated when a dilute amphiphilic aqueous solution and silica source are mixed. There is a positive interaction between the micellar aggregates and the silica species. As a result, the micellar aggregates will be covered with siliceous units. Eventually loosely aggregated flocs are formed. The floc is a concentrated phase of micelles and silica. The micelles are initially spherical or possibly slightly elongated. The flocs are spherical and thus isotropic. However with time, as the micelles grow into cylindrical shape, the flocs will become anisotropic (shaped more or less like an ice-hockey puck).[2] The height to width ratio of the 'puck' shaped particle varies depending on synthesis conditions.

In this work we have observed that the flocs, or primary particles, can, under certain conditions, specifically aggregate into larger units, so-called secondary particles. We have observed that the specificity of this aggregation can be controlled by synthesis temperature. The aggregation occurs while the primary particles are still quite liquid-like and this characteristic permits considerable rearrangment within the aggregates. The rearrangement can even allow formation of perfect mesoscopic single-crystal particles, even though holes or other types of defects frequently occur.

The specificity can as mentioned above be controlled by temperature and possibly also by other synthesis conditions. Here we have focused on the formation of secondary particles formed by sideways aggregation of the 'puck'-shaped primary particles. A normal synthesis leads to the formation of a seven-mer of primary particles (see figure 1.2). The secondary particle thus formed will have a size roughly seven times larger that the primary particle. Even though there is considerable rearrangemnet as the primary particles aggregate the thickness is conserved.
The aggregation occurs at a particular point in time during the synthesis. As this was identified from in-situ measurements[2] the synthesis path could be altered.[6, 7] It was demonstrated that the aggregation step could be modified in three ways[6, 7]:

1. It could be prevented - resulting in primary particles
2. The specificity could be lost – resulting in undefined aggregates
3. It could be enhanced – resulting in larger plate-like particles

Enhancing the aggregation leads to larger plate-like particles. Figure 1.2 shows the methodology (and terminology) used for these experiments. When the specific aggregation was prevented, 1st generation particles were obtained. A normal synthesis leads to a seven-mer, 2nd generation particles. If the aggregation was boosted (within limits), 3rd or 4th generation particles resulted. It should be stressed that the thickness, regardless of generation, is the same and also that the final particles are more or less perfect mesocopic single-crystals. The aggregating interfaces have more or less vanished due to the liquid-like nature of the particles at the time of aggregation.
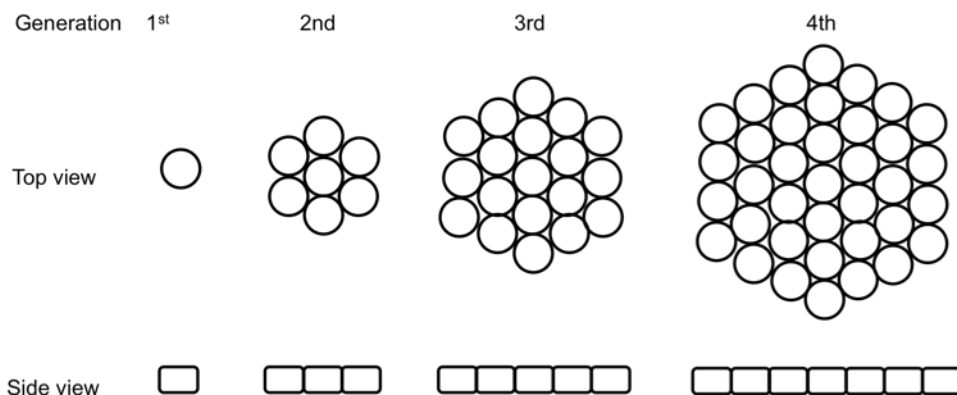
Figure 1.2. The sketch shows the different generations of particles. It is only the diameter that changes while the thickness is constant.

Thus, the necessity of knowledge and understanding of the formation of the materials can provide the scientist with a crucial "tool" to control the properties the materials. This thesis aims to contribute to filling of the current knowledge gap.

The thesis is divided in two parts. The first part aims to put the work in a bigger context, introducing the reader to surface and colloid chemistry and giving a background to mesoporous materials, introducing the techniques used and lastly giving a summary of the obtained results. The second part of the thesis contains the publications resulting from this PhD project.

2. Surface and colloid chemistry

Colloidal particles are particles ranging from 1nm to 1μm dispersed in a continuous medium. Such particles have a large surface area and the properties of the surface influence the behavior of the particles. Consequently, surface chemistry is an important aspect in colloidal science. This chapter aims to give the reader an introduction to the field of surface and colloid chemistry and its relevance to the formation of mesoporous SBA-15.

2.1 Amphiphilic molecules

An amphiphilic molecule is composed of at least two parts, one part that prefers the solvent and another part that does not. In an aqueous solution the two parts are referred to as either being hydrophilic or hydrophobic. Due to this, amphiphiles are often attracted to interfaces of two immiscible phases. At a water/oil interface the hydrophobic part is situated in the oil phase and the hydrophilic part in the water phase. The driving force of this behavior is to lower the surface free energy of the interface. Due to their preference to surfaces, such molecules are often called surfactants (surface active agents). [8]

2.1.1 Surfactants

Surfactants are the biggest group of amphiphiles and can be classified by the characteristics of their head group; anionic, cationic, zwitterionic and non-ionic surfactants. They all have a polar head group and nonpolar tail (Fig. 2.1a). The hydrophobic group is often a hydrocarbon chain. At low concentrations in water they occur as unimers, while with an increase of the surfactant concentration, aggregates can spontaneously form (Fig. 2.1b). Then, the critical micellar concentration (cmc) is reached. The cmc is a result of two competing factors. 1. Bringing the nonpolar chains out of the water phase and into an oil-like environment due to the so-called hydrophobic effect drives the micellization[9] 2. The repulsion between the polar headgroups opposes the formation of aggregates. Concequently, a non-charged head group and a longer nonpolar tail have a low value of the cmc whereas a charged headgroup and a short tail have a higher value. The nature of the surfactant, the surfactant concentration, the temperature, the salt concentration and the solvent conditions are other factors that influence the cmc and the geometry of the aggregate. A spherical shape of the aggregate is the most common at low surfactant concentration, but different geometries can arise. An increase in surfactant

concentration often results in an elongation of the aggregate. A further increase in concentration often leads to the formation of liquid crystalline phases. [10]
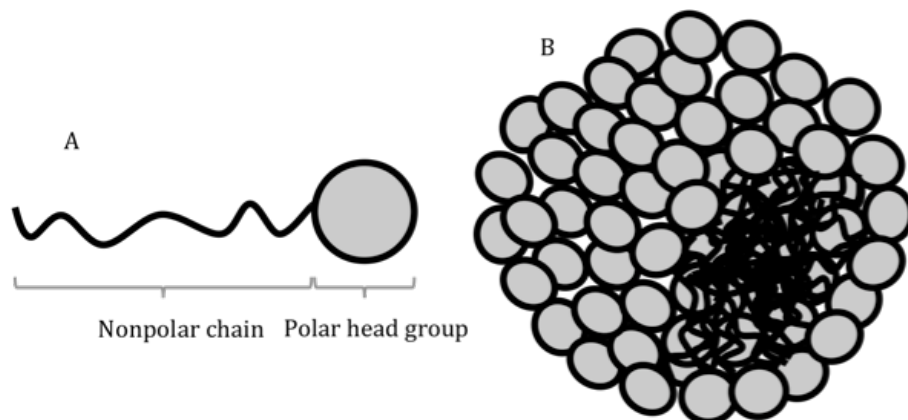
Figure 2.1. Schematic picture of a) a surfactant and b) micelle. The surfactants spontaneously form micelles above a specific concentration, the critical micellar concentration. The centre of the micelle can be regarded as an oil droplet.

2.1.3 Amphiphilic polymers

A polymer is a large molecule that is built up of smaller covalently bound repetetive units (monomers) in a linear or branched way. If the polymer consists of one kind of monomers it is called a homopolymer. The silica in the SBA-15 can be regarded as a highly branched homopolymer. At addition to the micellar solution the silica source is in a monomeric form, but after polymerzation it becomes a polymer. Polymers constiting of two or more monomers are defined as copolymers. There is a large number of copolymers that have amphiphilic properties. In order for a polymer to be amphiphilic it needs to be built up of at least two different types of monomers, one hydrophobic and one hydrophilic. If the two types of monomers are divided in blocks, the polymer is identified as a block copolymer. In this work, a non-ionic amphiphilic triblock copolymer with the trade name Pluronics was utilized. More specificly, the triblock copolymer Pluronic P104 ($EO_{27}PO_{61}EO_{27}$) was used in the synthesis of mesoporous SBA-15. The ethylene oxide (EO) part is considered, in this composition, to be hydrophilic and the propylene oxide (PO) part to be hydrophobic (fig. 2.2). As a result in solution, the triblock copolymer molecules form aggregates in a similar way as surfactants. There is a range of Pluronics with different EO/PO ratios. The EO/PO ratio changes the hydrophilicity/hydrophobicity character of the polymers and hence also affects the phase behavior of the polymers.

$$HO\text{-}(CH_2CH_2O)_x\text{-}(CH_2C(CH_3)HO)_y\text{-}(CH_2CH_2O)_x\text{-}H$$

Figure 2.2. Formula and a schematic picture of a Pluronic polymer. Aggegates are formed in aqueous solution above the critical aggregation concentration(cac).

Normally, solubility of substances increases with a higher temperature. However, the ethylene-based polymers exhibit an inverse temperature behavior. As the temperature increases the aqueous solubility decreases which can lead to spherical aggregates growing t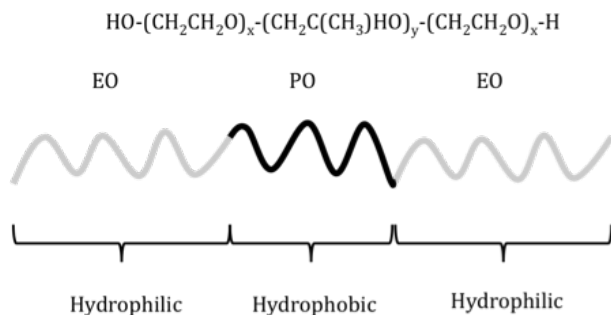o rods.[11] Karlström et al. proposed an explanation to this phenomenon. When increasing the temperature the configuration of the ethylene chain changes. The new conformation has a smaller or no dipole moment and hence the ethylene chains will interact less favorably with water.[12] Consequently, the ethylenebased polymer will eventually phase separate provided the temperature is high enough. The phase separating temperature, at a specific polymer concentration, is called the cloud point. At this point two phases are formed, one rich in polymer and one dilute polymer phase. A different approach to influence the phase behaviour of the ethylenebased polymer is to add different salts.[13] Both anions and cations have an effect on the phase behaviour. However, it is generally found that anions have a larger influence. Some anions show a preference to adsorb to the palisade layer of the micelles and thereby increase the solubility of the aggregate. The cloud point is then raised to a higher temperature. Other anions prefer being in the bulk solution and thereby making the solvent more polar. In this case, the cloud point decreases. The classification of ions regarding their ability to influence solubility is called the Hofmeister series. The polymer concentration also has an effect on the phase behaviour of the Pluronics and a phase diagram is a useful way of picturing this fact.[11,14] Pluronic water systems have a large structural diversity depending on concentration.

2.1.4 Surfactant number and curvature

Dilute amphiphilic solutions above the cmc or above the critical aggregation concentration (cac) give rise to aggregates with a specific geometry. Depending on the relative size of the non-polar tail and the polar head group different aggregate geometries are formed. The surfactant number N_s is a good way of predicting the geometry of the aggregate,

(2.1) $$N_s = \frac{v}{la_0}$$

17

where v and l are the volume and the length, respectively, of the hydrocarbon tail and a_0 is the effective area per head group. The volume (nm^3) and the length (nm) can be calculated according to

(2.2)
$$v = 0.027(n_c + n_{Me})$$

(2.3)
$$l = 0.15 + 0.27 n_c$$

where n_c is the number of carbons and n_{Me} correspond to the number of methyl groups. The most likely geometry when the surfactant number equals one third is a spherical aggregate. A slightly higher number, N_s=0.5, normally gives rise to a cylindrical shaped aggregate. A planar surfactant bilayer is obtained when the surfactant number is unity. Another way of describing the aggregate structure is to consider the mean curvature, H, of the surfactant film at an interface.

$$H = \frac{1}{2}\left(\frac{1}{R_1} + \frac{1}{R_2}\right)$$
(2.4)

where R_1 and R_2 equals the radii of curvature in two perpendicular directions. For a spherical geometry (R=R_1=R_2) and consequently H=R^{-1}. For a cylindrical object, where R_1=R and R_2=∞, H=$(2R)^{-1}$. [8]

2.2 Liquid crystals (LC)

High concentration of amphiphilic molecules, usually in water, may result in a lyotropic liquid crystalline phase (LC). The LC phases possess a degree of order intermediate between the molecular disorder in an isotropic solution and the regular structure of a crystal. Amphiphilic molecules in a LC have a long-range orientational order and a liquid like disorder on a molecular scale. Pluronic triblock copolymers PEO-PPO-PEO can form a range of LC phases, which is often illustrated in phase diagrams. The molecules are associated with weak physical interactions. It is hence possible to influence the phase behaviour by small changes in external factors such as temperature, concentration, salt addition etc. By varying the concentration of the amphiphile, different liquid crystalline phases can be generated. Normally, going from a low to high amphiphilic concentration, the following self-assembled phases are obtained: micellar solution, micellar cubic, 2D hexagonal, bicontinous cubic and lamellar (Fig. 2.3). The phases have different physicochemical properties, which can be utilized for industrial applications. Different phases can be identified by a number of techniques. An easy way of distinguish between phases is to use polarized light. Hexagonal, lamellar and other anisotropic structures are birefringent and give rise to characteristic textures. The isotropic cubic structures do not give rise to textures and cannot be distinguished from each other. Small angle scattering (SAS) and nuclear

magnetic resonance are two other useful techniques to characterize LC phases. The LC phases generate Bragg peaks at specific positions and hence from these positions it is possible to identify the phase. Small angle X-ray scattering will be discussed in more depth in the experimental section (section 4.1.1).
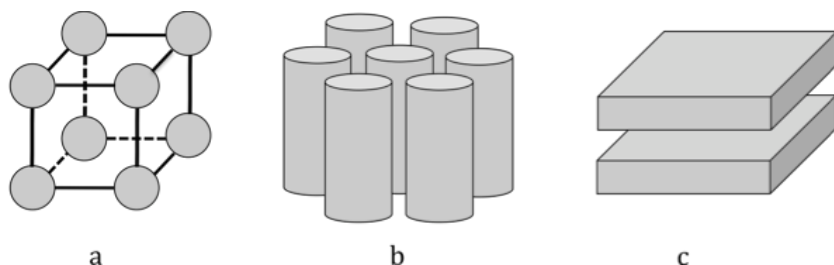
Figure 2.3. Schematic picture of possible LC structures a) cubic, b) hexagonal and c) lamellar. Solvent separates the grey objects (micellar aggregates). This thesis focuses on the 2 dimensional hexagonal structure.

There is another group of liquid crystals, which are called thermotropic. A thermotropic LC is induced by a change in temperature and may be classified based on their structure. In a nematic LC phase (Fig. 2.4b) the preferred orientation is homogenous throughout the system. A smectic phase also has a long-range orientational order as well as a long-range translational order in one or two directions (Fig. 2.4c). [15]
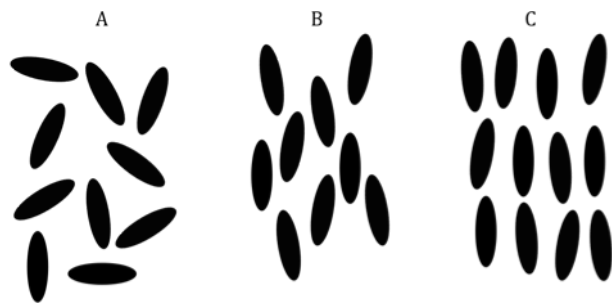
Figure 2.4. Different liquid crystal structures a) isotropic, b) nematic and c) smectic.

The formation of SBA-15 was roughly described in the introduction. The flocs are initially more or less isotropic. However, due to elongation of micelles inside the flocs the particle becomes anisotropic and the evolution goes through a nematic-like stage into an ordered particle.

2.3. Nucleation, growth and order

There are fundamentally two strategies of forming a colloidal dispersion, either by dispersion or by nucleation and growth process. In the dispersion method, large particles are mechanically divided into smaller ones. The nucleation method is more widely used and basically smaller molecules aggregate to form a colloidal particle. The particle formation of SBA-15 can be described with the nucleation and growth process.

2.3.1 Nucleation and Growth

Nucleation can be divided into heterogeneous and homogenous nucleation. The heterogenoeus nucleation is more common and occurs and at interfaces or impurities. Homogeneous nucleation takes place due to small fluctuations in the uniform bulk. For a nucleation to occur the concentration or vapor pressure needs to exceed the equilibrium value by a considerable amount. The system is then supersaturated. However, there is an energetic barrier for the phase transition. The cost in surface free energy of forming a new interface opposes phase transition, which makes the process sluggish. Equation 2.5 displays the free energy change of forming a particle of radius R. The first term shows the decrease in surface free energy by an increase in aggregate volume when forming a particle and the second show the increase in surface free energy of forming a new interface.

$$(2.5) \qquad \Delta G = -nkT\ln\left(\frac{c}{c_s}\right) + 4\pi R^2\gamma = -\frac{4}{3}\pi\frac{R^3}{V_s}kT\ln\left(\frac{c}{c_s}\right) + 4\pi R^2\gamma$$

where n equals the numbers of moles solute, k is Boltzmann's constant, T equals the temperature, c and c_s equals the solute concentration and the supersaturation concentration, respectively, V_s equals the solute volume and last γ is the free energy of the precipitate-solvent surface. If the formed nucleus is too small, the energy that would be released by forming its volume is not enough to create its surface, and nucleation does not proceed. If the radius of the nuclei is large enough the growth can start and thereby lower the free energy of the system. Consequently, there is a critical radius of the nuclei, the Kelvin radius, which decides the fate of the nuclei.

Figure 2.5 shows a schematic view of the nucleation and growth step. Nucleation occurs above the critical supersaturation concentration. To obtain monodisperse colloids the nucleation should be a fast burst. The time above the supersaturation point should be very short. The number of formed nuclei decides the size of the final particles. The formation of nuclei lowers the concentration below the critical supersaturation point and no more nuclei are formed. It is also important to separate the nucleation step and the growth step if monodisperse colloidal particles should be obtained. The growth of the nuclei continues until the concentration is lower than the saturation concentration. [8, 16, 17]
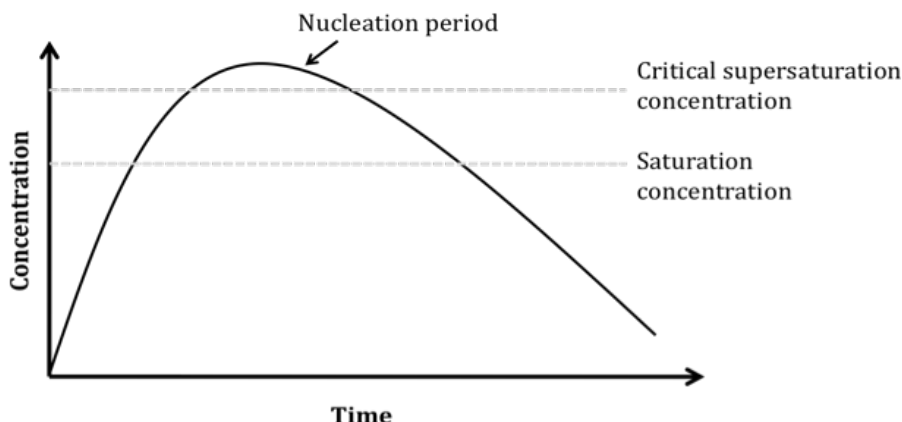
Figure 2.5. The nucleation occur above the critical supersaturation concentration (nucleation concentration). The number of formed nuclei define the number of particles. The nucleation stops below the critical supersaturation concentration and the growth of the nuclei start. The growth continues until the saturation concentration is passed.

Paper 1 describes the formation of SBA-15 as a nucleation and growth step. In the beginning of the synthesis the micellar collisions will not lead to an association. However, supersaturation is reached due to the continously adsorbing silica to the palisade layer and/or the ongoing silica polymersation in the palisade layer of the micelles. Eventually the nucleation barrier is passed and the formed nuclei are stable. The nuclei will then grow on the expense of the free micelles in solution. Primary particles are now formed and depending on synthesis conditions further aggregation and ordering of the mesophase take place. The obtained final particles are monodisperse, which indicate that the nucleation occurred in a single short burst and that the nucleation and the growth step are separated in time.

2.4 Colloidal stability

Interactions between colloidal particles in a dispersion are important in many perspectives, both from an academic and an industrial point of view. In order for dispersions to be stable some kind of repulsive force between the colloids is imperative. On the other hand, if the overall interaction is attractive the colloid aggregates will flocculate or coagulate. This will result in a phase separation.

2.4.1 Derjaguin-Landau-Verwey-Overbeek (DLVO) theory

The DLVO theory is a common way of describing the stability of a colloidal dispersion. The stability is, according to this theory, dependent on two competing forces, the repulsive energy due to an overlap of the electric double layers and an attractive van der Waals force. The potential energy as a function of distance between the particles is presented schematically in figure 2.6. If the energetic barrier is large

compared to the thermal energy (kT), a kinetically stable colloidal dispersion (2.6a). The other extreme is figure 2b, show an unstable colloidal dispersion. The attractive van der Waals interaction between colloids will lead to coagulation of the particles. The last curve illustrates a system that have two minima, a primary and a secondary minimum. If the energetic barrier between the minima is large compared to kT and the secondary minima is comparable to kT, the particles can flocculate. The flocculation is revesible and the weakly bound particles are called flocs. If the particles are situated in the deeper primary minimum, the particles coagulate, in an irreversible process.[8, 15, 17]
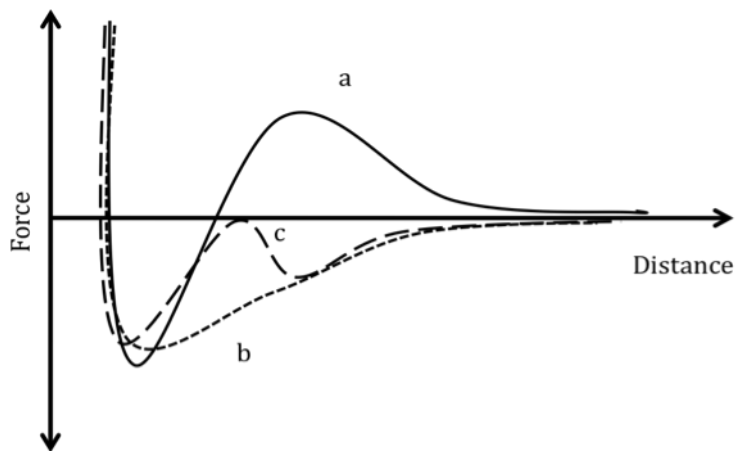
Figure 2.6. The solid curve a) shows a kinetically stable colloidal dispersion. The b-curve displays an unstable dispersion. The colloidal particles will coagulate. The intermediate case, the c-curve, shows a system with two minima. If the kinetic barrier is larger than the thermal energy, the particles will end up in the secondary minima and hence flocculate

There are a number of ways of destabilizing a colloidal dispersion. Addition of salt or/and polymer are two ways of coagulate/flocculate the system. However, polymers often stabilize a colloidal dispersion. The stabilizing/destabilizing polymer effect depends on the polymer concentration, whether or not the polymer adsorb to the particle surface, the degreee of coverage and the solvent conditions.

2.4.2 Steric repulsion

A colloidal dispersion can, as mentioned above, be stabilized by addition of polymers. In that case a part of the polymer needs to have a higher affinity to the colloidal surface than to the solvent and thereby adsorb to the surface. The other part of the polymer is sticking out from the surface. It is also possible to attach the polymer by grafting. Block copolymers, with one hydrophilic and one hydrophobic part, are usually good stabilizers. It is important that a significant part of the surface is covered with polymer, otherwise an attraction between particles can occur (see next section).

The adsorbed layers of polymer prevent the colloidal particles to come in close contact. When particles approach the mobility of the "sticking out" polymer-chains will decrease. The decrease in configuration possibilities results in a decrease in entropy (or an increase in osmotic pressure) and an increase in Gibbs free energy of the system. Consequently, a repulsion force between the particles results. The solvent quality, with respect to the polymer, also influences the steric stabilization. In a good solvent, the polymer will be more stretched out and as a result be a better stabilizer. On the other hand, in a poor solvent the polymer layer will be more compact around the colloids and can in fact induce an attraction. In this case, as two surfaces approach each other, a polymer chain from one colloid can adsorb to the other. This lead to an increased configurational entropy and hence an attractive force. It could be seen as a form of bridging attraction.

2.4.3 Bridging attraction

An attraction, due to polymer adsorption, between colloidal particles take place if the polymer chain adsorbs to two or more particles. This induces a flocculation and is called bridging attraction. For this to happen the surface of the colloids can only be partly covered with polymer and the polymer needs to be long enough to span over the interparticle distance. A larger polymer and bad solvent conditions promote bridging flocculation.

2.4.4 Surface energy

The total surface free energy of particles in solution can be used to determine wether the particles are stable or not. The total surface free energy G_s of a particle can be calculated from the surface tension of the interfaces times the area of the interfaces. If an anisotropic liquid crystalline phase is considered the interfaces perpendicular and parallel to the aggregate direction will have a different molecular geometry and hence the surface free energy of the interfaces are most likely different. The surface free energies of the interfaces can be estimated by considering the details of the interfaces and hence the stability of the system.

A model was proposed in paper V explaining the morphology of hexagonal prismatic SBA-15 particles. The particles goes through a nematic like phase and hence the flocs are anisotropic due to the elongation of the micelles inside the flocs. The interface of the SBA-15 particles consist of cylindrical Pluronic aggregates with adsorbed silica oligomers/polymers. As a result the surface tension of the faces perpendicular and parallel to the direction of the micellar aggregates are different. The overall surface free energy of the particle determine the morphology of the mesoporous particles. If the volume of the floc is constant and if there is enough flexibility within the particle, the particle will adopt a specific height/width ratio. Moreover, at extreme synthesis temperatures the particles aggregate in an oriented way to reduce the overall surface free energy.

3. Mesoporous silica

3.1 Introduction

Mesoporous materials was first synthesised and reported in the beginning of the nineteen nineties[18-21] and this was the start of a very active research field. According to IUPAC, the pore diameter of mesoporous materials range from 2 to 50 nm. However, the mesoporous materials have normally a pore diameter around 2 and 30 nm. Materials with pores smaller than 2 nm are called microporous and materials with pores larger than 50 nm are called macroporous. Zeolites are included in the former group of materials. Despite the classification, some mesoporous materials not only have mesopores but also contain micropores. In contrast to zeolites, mesoporous materials are amorphous on the atomic scale and ordered on the mesoscopic scale. The mesoporous materials have a narrow pore size distribution, a very high surface area (800-1000 m^2/g) and are mechanically stable. Furthermore, the particles have in some cases a well-defined shape and size. These properties make the materials interesting for several applications for instance in catalysis[22], in separation processes[23], as carriers[24] and so on. There are a number of different types of mesoporous materials and today, many different ways of synthesizing them, which will be discussed below. Additionally, the use of different metal oxides in the synthesis can alter the surface and material properties. Titanium oxide, alumina oxide etc are used, but the most common inorganic, awhich is also the investigated in this work, is silicon dioxide. Only syntheses based on silica will be discussed

3.2 Synthesis methods

In all synthesis methods of mesoporous silica, an amphiphile, typically dissolved in aqueous solution, is used as structure directing agent and the synthesis is initiated as a silica source is added to the reaction solution. The silica source will polymerize around the amphiphilic aggregates and hence build up the walls in the forming structure (Fig 3.1). A common method, which is used in this PhD project, of synthesizing mesoporous materials is to start with a dilute amphiphilic (2.5 wt%) aqueous solution. An appropriate temperature is choosen and a silica source is added to the solution under vigorous stirring. The polymerizing silica interacts with the amphiphilic aggregates, which eventually will result in an precipitation. The synthesis solution is left for 24 hours on the bench before it is hydrothermaly treated in an oven at 80°C for another 24 hours. It has been found that the mesoporous structure and particle morphology are formed, depending on synthesis conditions, whitin the first hour of the synthesis. The hydrothermal step is performed to achieve a higher

connectivity of the silica. The precipitate are then filtered, washed and dried. The porous structure is obtained by removing the stucture directing agent/amphiphile from the pores by calcination or ethanol extraction.
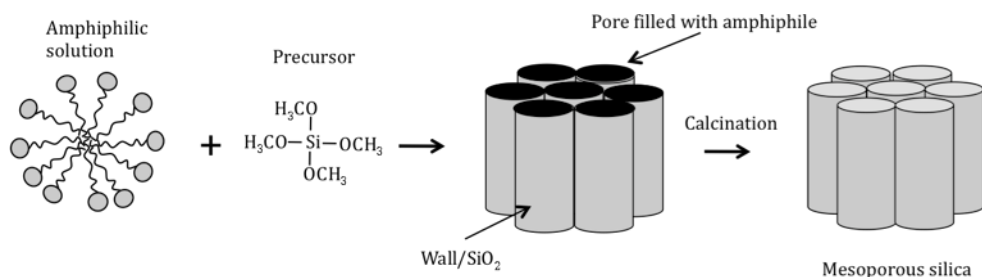

Figure 3.1. Schematic image of the synthesis procedure of mesoporous silica. An amphiphilic solution and a silica precursor are mixed at certain synthesis conditions. In due time an ordered material is formed. To obtain the porous structure the amphiphile is removed by calcination.

True liquid crystal templaring (TLCT) is another method to produce mesoporous materials[25]. In contrary to the previous method, a high ampiphilic concentration, 50 wt%, is used. A silica source is added to the already present liquid crystalline phase, which with time results in an ordered phase. However, inhomogenities in the material may result from inadequate diffussion of the silica source. Brinker et. al. proposed a third method, evaporation induced self assembly (EISA)[26]. An amphiphile is dissolved in water, ethanol and silica. The surfactant concentration is initially below the cmc but increases as ethanol evaporates. This will induce an ordered liquid crystalline phase. Different macroscopic morphologies can be obtained by EISA. For example, thin films can be obtained by dipcoating or spheres can be obtained through an aerosol based process. From now on, the focus will lie on the synthesis method applied in this thesis; the dilute solution method.

3.3 Structure directing agents

The structure directing agent is a fundamental ingredient in the synthesis of mesoporous silica and is responsible for the mesoscopic ordered structure. There are a number of different types of structure directing agents used in the formation of mesoporous materials and the most common ones will be discussed here. Exxon Mobil Corporation introduced a cationic surfactant, hexadecyltrimethyl-ammonium chloride (CTACl), in the synthesis of mesoporous silica.[18, 20] The M41S family was developed by varying the concentration of CTACl in the synthesis which lead to several structures. The material known as MCM-41 (2D-hexagonal), MCM-48 (cubic Ia3d) and MCM-50 (lamellar) were formed. The M41S materials have a pore size of 1.5-10nm and contain no microporosity. Triblock copolymer as structure directing agent belongs to another family of materials, and are ogten referred as SBA materials [1, 27]. 2D-hexagonal (SBA-15) and cubic Im3m (SBA-16) were synthesised

when the nonionic triblock copolymer Pluronics was utilized. The nononic templated SBA materials have, not only, a larger pore size (4-15nm) and thicker walls than the M41S materials, but also micropores. The micropores are a result of ethylene oxide chains trapped in the silica matrix. Recently, an anionic surfactant was used as structure directing agent. These materials belong to the AMS family (Anionic surfactant templated Mesoporous Silica)[28]. The AMS materials have shown to have a very large diversity regarding mesoscopic structures as a function of synthesis conditions.

In this thesis, a nonionic triblock copolymer was used as structure directing agent in the synthesis of hexagonal SBA-15. In that perspective, the focus will hence lie on the non-ionic amphiphilic directed synthesis.

3.4 Silica chemistry

The silica source is another essential component in the synthesis of mesoporous silica. There are number of available precursors and silicon alkoxides are the most common ones. Tetramethyl orthosilicate (TMOS) (fig. 3.1), tetraethyl orthosilicate (TEOS) and tetrapropyl orthosilicate (TPOS) are three examples of alkoxides. These alkoxides are fairly expensive and cheaper precursors, sodium silicate and fumed silica, can also be used in the synthesis of mesoporous silica.

$$H_3CO-\underset{\underset{OCH_3}{|}}{\overset{\overset{H_3CO}{|}}{Si}}-OCH_3$$
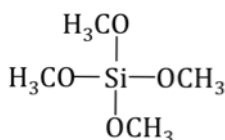
Figure 3.1. Chemical formula of the precursor TMOS.

In aquoues solution, the silicon alkoxides, hydrolyses (rxn i) and polymerizes (rxn ii & iii). In the end, a silica gel network is formed. Both steps are pH dependent and the silica kinetics can be varied with addition of acid or base (isoelectric point for silica is around pH 2). The hydrolysis is fast while the polymersation rate is slow for silicon aloxides in a aqueous solution of pH 2. Furthermore, the hydrolysis step is slower with a longer alkyl chain. The silica kinetics can also be contolled with for example catalysts such as F^-.[29-31]

i) Hydrolysis $\quad\quad\quad\quad \equiv Si - OR + H_2O \Leftrightarrow \equiv Si - OH + ROH$

ii) Alcohol condensation $\quad \equiv Si - OR + HO - Si \equiv \Leftrightarrow \equiv Si - O - Si \equiv + ROH$

iii) Water condensation $\quad \equiv Si - OH + HO - Si \equiv \Leftrightarrow \equiv Si - O - SI \equiv + H_2O$
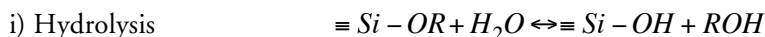
In this PhD project, mainly tetramethyl orthosilicate (TMOS) (Fig. 3.1) and in some cases tetraethyl ortosilicate (TEOS) and tetrapropyl orthosilicate (TPOS) were utilized as silica sources.

3.3 Synthesis of SBA-15

2D hexagonally structured SBA-15 was first synthesised in Santa Barbara.[1, 27] In the original synthesis recepie a small amount of Pluronic P123 was dissolved in hydrochloric acid. The concentration of Pluronic is around 2.5wt% and concequently above the critical micellar concentration. The temperature was set to 35°C and TMOS was added under vigorous stirring. This resulted in the hexagonal material SBA-15. SBA-15 can be synthesised with other types of Pluronic, at different temperatures, using other silica sources and even with additions of salt. The conditions can be varied and still the hexagonal structure is obtained but typically the lattice parameter changes with synthesis conditions.

In this thesis the slightly more hydrophilic amphiphile Pluronic P104 was used. The synthesis temperature was varied between 45 and 70°C and TMOS was, in most syntheses, used as a silica source. In a few syntheses salts were added prior to addition of the silica source. In all cases a well defined hexagonal structure was obtained and in most cases also a homogenoeus particle morphology and size. Figure 3.2 show the particle shape and the ordered structure for a 50°C synthesis.
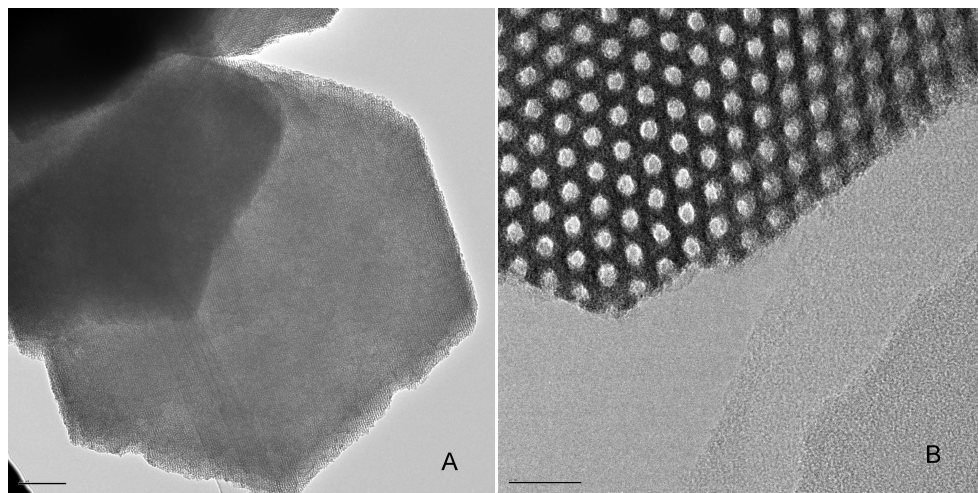

Figure 3.2. Transmission electron microscopy image of a) a SBA-15 particle and b) the hexagonal order of SBA-15. Scale bars: a) 200nm and b) 20nm

3.4 Mesoscopic order and particle morphology

The focus of this thesis is as previously metioned on the hexagonal ordered material, SBA-15. However, other mesoscopic structures (cubic Ia3d and Im3m, lamellar and 3-d hexagonal etc.) can be syntheseized with Pluronics as structure promoters, by small variations in synthesis conditions. The EO/PO ratio influence the mesoscopic order and can be used to control the outcome of the synthesis[1]. A higher EO/PO ratio promote micellar cubic order, while a lower EO/PO ratio normally result in a lamellar structure.[32, 33]. Moreover, the number of PO units has an influence on the pore size. A large number of PO segments and concequently a larger micellar core give rise to material with a larger pore size. In contrast, longer EO-chains give rise to material with a thicker wall. The Pluronic based polymers are known to be temperature sensitive as previously mentioned, and this fact can be used to tune both pore size and mesoscopic order.[33] Salt addition was also shown to have an effect on the block copolymer phase behaviour[13] and hence the mesoporous materials. Pluronic P123 normally promote a hexagonal structure. However, addition of 1M of sodium iodide to a Pluronic P123 solution promotes a cubic Ia3d structure.[34]. This cubic structure was also developed by addition of butanol at a sligthly higer pH.[35]. Kleitz et. al. also produced the cubic structures Im3m and Fm3m by adjusting the butanol/TEOS ratio.[36] The additions of salt and butanol along with the temperature changes, influence the packing parameter of the surfactant and thereby the outcome of the final material. The understanding of how and why the mesoscopic order can be altered is to some extent known, while there is a lack of knowledge of controlling/understanding the morphology of the particles. The final material can be highly ordered on the mesoscopic scale but have an undefined particle morphology. A well-defined particle morphology can be of importance from an industrial point of view. The same parameters which influence the mesoscopic order, have an effect on the macroscopic scale. The particle morphology can be tuned to give rise to different geometrical shapes. In the literature elongated, spherical, films, fibers, tubes, platelets etc. particles have been reported.[6, 37-39]. Zhao et. al. concluded that the competition between the free energy of the mesophase formation and the free energy of the surface free energy of the liquid crystal like phase determine the particle morphology. In paper V we present a model based on the surface energies of the defining faces and relate this to the observed morphologies for a range of conditions.

3.5 Proposed mechanism of formation of SBA-15 in literature

The formation mechanism of mesoporous materials has recieved some attention within the last ten years or so. However, the whole picture is still not resolved. Zhao et. al., initially suggested that the driving force is due to electrostatic, hydrogen bonding and van der Waals interaction between the charged EO units (S^0H^+) and the cationic silica species (I^+), $(S^0H^+)(Cl^-I^+)$. Since then, a number of publications regarding the formation mechanism have been published. A better understanding of how and why these materials form can lead to new and improved materials, hence it is

an important subject to study. However, some disagreements exist regarding how these materials are formed. One difficulty, when comparing results from different studies, is due to differences in synthesis conditions (acid, pH, silica source, temperature, Pluronic etc.). Here I will summerize the two views on the formation of SBA-15 material, indicating which synthesis conditions as well as which characterization techniques that have been used. Not all details will be considered here and interested readers are encouraged to read the publications.[40-42] I have also choosen to discuss results I believe is related to my system and this work. Hence this is not a exhaustive summary. Today, there are, more or less, two ways of describing the process.

1. The formation mechanism has been described as a nucleation and growth process or a colloidal phase separation.

Yu et. al. is one of few that have focused on the formation process of SBA-15 in the colloidal size region.[40] Pluronic P123 was used as structure directing agent and potassium chloride was added to the Pluronic solution giving a final concentration of 0.5M. The synthesis temperature was set to 38°C and TEOS was used as silica source. Samples were collected at different times after precipitation, removed by filtration and washed with water and ethanol to remove surfactant and unreacted silica. SEM images show initially aggregates smaller than 100 nm. TEM images show that the aggregates contain wormlike micelles but no hexagonal order. The aggregates eventually become long rods(curved and straight) and after 1 hour only straight rods are observed. Their proposed mechanism includes three stages. First, surfactant/silica aggregates are formed. Second, a liquid crystal like phase is formed when surfactant/silica aggregates interconnect. As the silica condenses further the new liquid phase grow denser and eventually precipitate. Last, the liquid crystal like phase grows further.

Flodström et. al., investigated the formation mechanism of SBA-15, with in situ time resolved SAXS study[41] and with time resolved NMR and TEM study[42]. Pluronic P123 was used as structure directing agent and the synthesis temperature was set to 35°C. Two different silica sources were used, TMOS (both articles) and TEOS (only in the SAXS study), respectively. For the time-resolved TEM study, a small volume of the synthesis solution were collected at different times. These volume solution were diluted with Millipore water to hinder the silica polymerization and the aggregation processes before being analyzed. The TEM images show that spherical micelles are encapsulated and held together with polymerizing silica, in flocs, just before precipitation is observed. With time, the micelles become elongated and eventually the hexagonal ordered phase is observed. In the time resolved ^{1}H NMR experiments the signal from the protons of the propylene methyl groups was recorded with time. The broadening of the peak is investigated, which indicate floc formation. The spherical micelles grow into cylindrical micelles inside the flocs and eventually are a hexagonal order formed. The time resolved in-situ SAXS article show spherical micelles until the hexagonal ordered phase appears. The study showed that hydrolysed

silicate species adsorb to the EO-part of the spherical micelles. Further, elongation of micelles and parallel formation of hexagonal order take place inside the flocs.

This thesis is a continuation of the studies[41, 42] regarding SBA-15. Both the nanometerscale as well as the micrometerscale have been investigated. However, the focus is less on the developing mesoscopic structure but rather on the colloidal aspects of formation of SBA-15. The results from the thesis can be found in chapter 5.

Mesa et. al. used DLS (dynamic light scattering) and optical microscopy to monitor the evolution of the Pluronic P123 micelles in hydrochloric acid and TEOS solution.[43] The authors have a lower HCl concentration (0.4M) and lower amount of Pluronic (0.79 wt%) than normally used in the SBA-15 synthesis[1]. Mesa et. al. describe the formation of SBA-15 as occuring in three steps. First, silica adsorb to the EO-layer and this has two consequences, an increase in micellar size and a decrease in zeta potential. This is explained as a result of the adsorbed silica screening the protonated EO groups and, at some point, the silica coated micelles become unstable. Second, the decrease in zeta potential induces the phase separation. The silica coated micelles will fuse together and thereby form liquid like micron size particles. The last step concerns the solidification of the liquid particles.

2. Micelles grow into long cylinders which then aggregate. The aggregation and the appearance of the order happen concomitantly

Ruthstein et. al. have used electron paramagnetic resonance (EPR), electron spin-echo envelope modulation (ESEEM) and cryo transmission electron microscopy (cryo-TEM) to investigate the formation of SBA-15.[44-46] The synthesis procedure used was according to Zhao et. al.[1] recipie, with the exception ofn in some cases, using orto-phosphoric acid instead of hydrochloric acid and addition of a spin probe to the micellar solution. The synthesis are thus performed at higher pH and with other anions present, which slows down the kinetics. The EPR in combination with ESEEM makes it possible to monitor the interactions between ethylene oxide chains and silica. Changes in polarity and water content as well as the tumbling rate of the Pluronics are investigated. The analyses of the EPR and ESEEM results[44, 45] indicate three stages in the synthesis, 1) TMOS penetrate into the core of the micelles with a simultaneous hydrolysis. Water, methanol and more or less hydrolysed TMOS diffuse in to the corona. 2) The hydrolysed TMOS polymerise at the core/corona interface. 3) No changes in the core region was detected, while the silica polymerzation continues in the corona. The EPR and ESEEM reports were later compared with a cryo-TEM study[46]. The EPR and ESEEM work focus on the molecular length scale, whereas the cryo-TEM results concentrate on the mesoscopic length scale. The same system as in the EPR and ESEEM publications was investigated. However, the authors also, for comparison, investigated a SBA-15 synthesis made with hydrochloric acid at a slightly lower temperature. Pluronic P123 was used as structure directing agent and TMOS was used as silica source. The authors collected the reaction mixture regularly during the synthesis and investigated the system with cryo-TEM. It was concluded that the micelles elongate with addition of TMOS. The micelles

further grow into thread-like micelles of up to 700 nm. The thread like micelles become longer and stiffer and eventually form bundles. The hexagonal ordered phase appear as the thread-like micelles aggregate. The results are in agreement with another synchrotron SAXS study.[47]

Khodakov et. al. published an in situ time resolved SAXS study on the formation of SBA-15.[47] Pluronic P123 as structure directing agent, TEOS as silica source and a synthesis temperature of 40°C were used. Amount of TEOS and pH were varied. No micelles prior the addition of TEOS were detected, but it was infered that the micelles are of spherical shape initially and then elongate and form cylindrical micelles. At some point, the data could not be satisfactorily fitted, which could be due to presence of mixed micellar system. Eventually the cylindrical micelles pack in a hexagonal ordered structure. The same group published a time resolved in situ SANS study of a same system.[48] They detect spherical micelles, which become cylindrical and then pack in a hexagonal order. The authors also state that the precipitation is associated with the self-assembly of cylindrical micelles. Consequently, the precipitation occurs at the same time as the (10) peak appears.

Earlier this year Sundblom et. al published an in situ SAXS study on the formation of SBA-15. In this work, they developed a model to analyze the whole synthesis event, both the scattering part as well as the diffraction part.[49] P123 was used as structure directing agent and prehydrolysed TEOS as silica source. The pH of the solution was set to 2-3 and the synthesis is performed at room temperature in order to decrease the fast evolution of the material. The results show an elongation of spherical micelles into cylinders. The cylinders then aggregate and form a hexagonal phase.

3.6 Application

A reason for the very active research field of mesoporous materials is their potential use in industrial applications. The high surface area, narrow pore size distribution, chemical and mechanical stability along with large pores makes the material interesting for several application. Catalysis and separation methods are two areas, where the materials have been applied. However, the mesoporous materials have shown potential usage in other areas such as in electronics, for controlled release, in optical devices and for biological applications. For example, mesoporous silica materials has shown to have a considerably lower dielectric constant than traditional silica chips.[50] Additionally, a lot of work has been done to functionalize the material, e.g. attach organic components onto the silica matrix. This could open up for applications in host-guest systems. There are a number of reviews covering the potential use of mesoporous materials.[51, 52]

4. Experimental techniques

A number of techniques have been used for the work presented in this thesis. In this section the techniques used in the papers are discussed.

4.1 Scattering

4.1.1 Small angle X-ray scattering/diffraction (SAXS/SAXD)

SAXS/SAXD is an useful tool to characterize systems in the size region of 1-100 nm. A scattering pattern (Fig. 4.1a) is the result from a diffuse scatterer and a diffraction pattern (Fig. 4.1b) is obtained when the sample is ordered. For example, a dilute micellar solution give rise to a scattering pattern, while a liquid crystalline order of the same surfactant system gives rise to a diffraction pattern. SAXS/SAXD is an ideal technique to follow the evolution of the mesoporous structure.
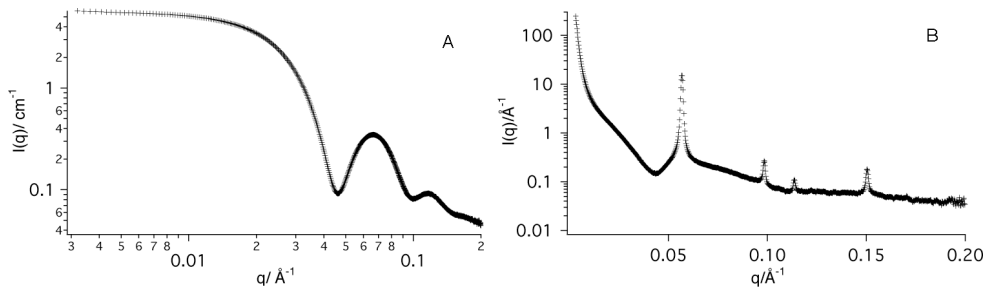

Figure 4.1. Two diffractograms obtained from a) SAXS and b) SAXD measurements.

X-rays interact with the electrons in the sample and are scattered *i.e.* deviates from the direction of the incident X-ray beam. The nonuniform distribution of electrons, the electron density, in the sample give rise to a characteristic pattern. Moreover, the greater the difference in electron density between parts of the sample, the bigger is the contrast and hence the structure can be more clearly resolved. If the electron density is more or less uniform in the sample, the scattering pattern is very weak. Normally, as in figure 4.1, the intensity is plotted against q. The q-vector is defined as the difference in the scattered vector $\vec{k}_s$ and the incoming vector $\vec{k}_i$ of the X-ray beam (Fig 4.2).
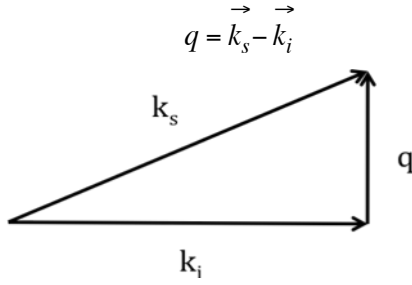
Figure 4.2. The definition of the scattering vector q

The magnitude of the vectors are both equal to $2\pi/\lambda$. If we assume elastic scattering *i.e.* no changes in energy between the incoming and the scattered wave, the q-vector can be expressed as

$$\vec{q} = \frac{4\pi}{\lambda}\sin\frac{\theta}{2}$$

(4.1)

where λ equals the wavelength of the X-ray beam and θ is the scattering angle.

The intensity I(q) can be as expressed as

(4.2) $$I(q) \propto P(q)S(q)$$

where P(q) is the form factor and S(q) is the structure factor of the material studied. P(q) depends on the size and the geometry of the scattering object, while S(q) depends on the interactions between the scattering objects. In a dilute solution, S(q) can be considered to be 1 and hence the scattering curve depends only on the form factor.

The scattering vector q probes a characteristic distance d in the sample

(4.3) $$d = \frac{2\pi}{q}$$

In the case of an ordered system (fig. 4.3), Bragg peaks can appear. The position of the Bragg peaks reflects the symmetry of the structure. The peaks appear due to constructive interference when the diffraction angle of the beam satisifies Braggs law

(4.4) $$n\lambda = 2d \cdot \sin\theta$$

where n is the order of diffraction, d is the spacing between lattice planes.
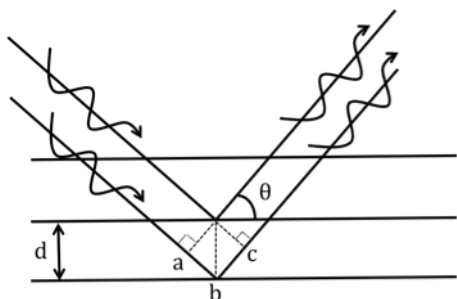
Figure 4.3. Schematic picture of refleclection of X-rays of an ordered phase. Constructive interference occur if the distance abc equals an integer number of the wavelength.

Constructive interference of the waves arises when the difference in path length (abc in figure 4.3) equals an integer number of wave lengths (nλ).

The unit cell is the smallest repeating unit of a crystalline structure. Figure 4.4 display the d-spacing and the cell parameter for a hexagonal phase. For a hexagonal liquid crystalline phase the distance between the cell parameter a, that defines the unit cell, can be calculated from the the first Bragg peak position, $a = \dfrac{2}{\sqrt{3}} \dfrac{2\pi}{q_1}$
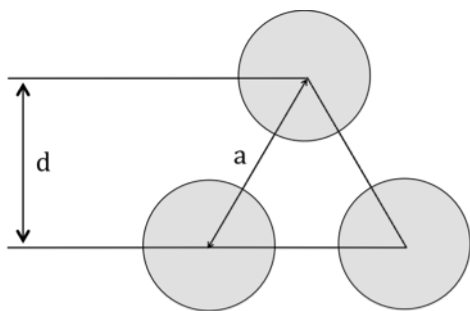

Figure 4.4. Schematic picture of a hexagonal phase with the characteristic d-spacing and the unit cell parameter a.

Normlly, Miller indeces is used to describe the structural arrangement for a specific phase. [8, 15, 53]

To perform time resolved mesurements of a continuously changing system is a challenging task. If the rate of the kinetics is high, a special set up might be needed. A synchrotron source provide a very high flux of X-rays, much more powerful than an in-house SAXS that can be found in many labs. With a synchrotron source the time to obtain a well resolved diffractogram is much shorter and it is possible to collect diffractograms more frequently. Time resolved in situ SAXS measurements were

performed at the ID02 at the European synchrotron radiation facility (ESRF) in Grenoble, France and at the Austrian SAXS-beam line at ELETTRA in Trieste, Italy.

4.1.2 Ultra small angle X-ray scattering (USAXS)

Whereas SAXS monitor objects on the nanometer scale, USAXS can be used to study objects in the order of several micrometers. The time resolved in situ USAXS measurements in this PhD project were performed at ESRF. A Bonse-Hart camera with crossed crystal analyzer configuration extends the low q-limit to 8e-4 nm^{-1}, which in theory would allow the study of objects up to 7-8 μm. However, the USAXS suffer from slower acqusition time and hence fast kinetic systems is not optimal to measure. The instrument scan over a range of angles to collect data sequentially. The USAXS measurements were peformed at ESRF and the acqusition time was around 2 minutes and 45 seconds.

4.1.3 Small angle neutron scattering (SANS)

Similarly to SAXS, described earlier, SANS gives information on the scale from 1nm to 100nm. The same priniciples as for SAXS can be applied to SANS. The major diffrence is that X-rays, as mentioned, are scattered by electron clouds surronding the nucleus while neutrons are scattered by the nucleus itself. The scattering length density of a substance characterize the interaction between the nucleus and the neutrons. For example, hydrogen and deuterium have a very different scattering length density, which can be used. If water is used as a solvent the scattering length density of the solvent can be varied by mixing H_2O and D_2O. It is then possible to specificly investigate parts of the sample. This is referred to as contrast matching and exemplified in figure 4.5.[53]
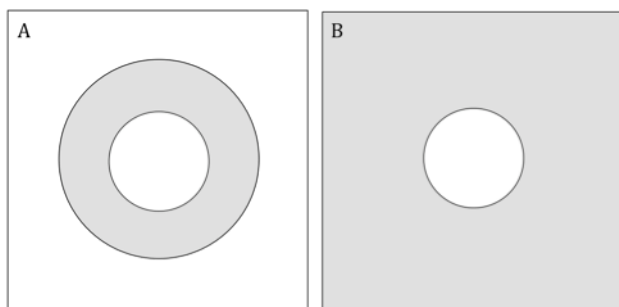

Figure 4.5. An example of contrast matching of a sample containing spherical micelle in an aqueous solution. Since hydrogen an deuterium have very different scattering length density it is possible to mix H_2O and D_2O so the scattering length density correspong to a scattering length density of another part of the sample. In a) the scattering length density for the solvent and the the micellar core is identical and as a results only the palisade layer can be investigated. On the other hand, in b) the scatterig length density for the solvent and the palisade layer is identical and hence only the core give rise to a scattering pattern.

SANS measurements were performed on NG3 and NG7 at NIST centre for neutron research in Gaithersburg, USA and on D16 at ILL in Grenoble, France.

4.2 Electron microscopy

X-ray scattering identify the overall material properties as the unit cell parameter or particle shape. Electron microscopy, on the other hand, can also visualize details in the structure, variations in the unit cell parameter, defects and morphology of the particles.

4.2.1 Transmission electron microscopy (TEM)

TEM is used to image crystallographic structures of samples and can in principle be used down to the atomic level. A TEM microscope is a complex and expensive piece of equipment but an important technique to characterize structural properties. Briefly described, an electron gun emits electrons which passes through a sample and are then projected onto a electron sensitive detector. Electromagnetic lenses are used to focus the beam. The objective lens forms the image, the projector lenses enlarge the image and projects it on the screen or the image recording device (often a CCD-camera). A HRTEM can have a resolution of Ångström and consequently analysis on the atomic level can be performed. One should keep in mind that TEM produces a 2D image of a 3D object. Moreover, TEM equipped with other analysis equipment, for instance an EDS-system, can be used to do elementary analyses. Electron diffraction can also be performed on ordered materials, giving information regarding order and lattice spacing. TEM is performed on solid samples, while cryo-TEM is applied on liquid samples.[54] The materials studied here were dispersed in acetone and then dropped onto holey carbon cupper grids before analysis in the TEM.

4.2.2 Scanning electron microscopy (SEM)

SEM is normally used for morphology investigations and hence an image with 3-d information of the sample is obtained. The resolution for a SEM is around 1nm. In a SEM, an electron gun emits electons that scan the sample. The detectors collect inelastic secondary alectrons as well as back scattered electrons, which are then amplified. The scattered inelastic secondary electrons are used to build up a 3D image, while the back scattered electrons can be used to analyse the composition of the sample. In order to reduce charge effects, which normally occur for insulating materials such as silica materials, the sample is coated with a thin layer of a conducting material. In this project, the samples was coated with gold before analysis with SEM. However, for detailed investigation of a surface, an uncoated sample is preferred. Another prerequisite to reduce the charge effects is to investigate single particles. Several aggregated single particles give rise to charge effects and hence a less resolved image.[55]

4.2.3 Electron tomography

Electron tomography is used to obtain a 3D image of the sample. Basically, the 3D structure is reconstructed from a series of projected TEM 2D images, taken at different tilt angles. The electron beam is scanned over an area of the sample and the technique is refered to as scanning transmission electron microscopy (STEM). In paper V, STEM HAADF was performed on a couple of samples tomographic reconstructions. HAADF is the short version of "high angel annular dark field" and the detector collects incoherently scattered electrons. The resolution is around 1nm.[56, 57]

4.4 UV/VIS spectrophotometer

Small things dispersed in water appear to the eye as transparent. A high concentration of larger objects dispersed in water scatter visible light and hence the dispersion is non-transparent. Spectrophotometers can be used to monitor changes in turbidity of a sample with time. The spectrophotometer measurements on the turbidity used in this work is a qualitative and hence can not be correlated to a specific concentration. A spectrophotometer measures the intensity of light passing through a sample and compares it with the intensity of the light of the incoming beam. The higher the intensity of scattered light, the higher is the turbidity. In paper 2, turbidity measurements as a function on time were performed on samples to deduce the onset of the nucleation and growth of particles. Larger particles, if the refractive index of the particles is different from the refractive index of the solvent, scatter more visible light and hence the turbidity increases.

5. Summary of results

The results obtained for this thesis are here divided in two categories. One concerning the formation mechanism of SBA-15 (paper I-V) and one describing how the material properties can be altered and controlled if knowledge about the formation mechanism is available (paper VI).

5.1 Colloidal aspects of formation mechanism (I-V)

The SBA-15 material was synthesised according to the synthesis reported by Zhao et. al.[1], with some minor exception. The sligthly more hydrophilic triblock copolymer P104 was used instead of P123. The syntheses were performed (paper I, II, V and VI) with varying temperatures, from 50 and 65°C, in steps of 5°C (Fig 5.1).
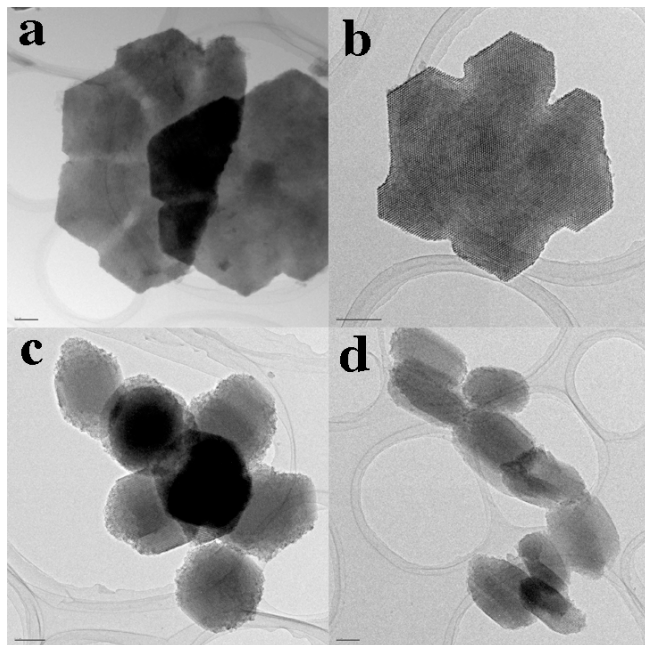

Figure 5.1. TEM image showing the investigated system. The particles were formed at a) 50, b) 55, c) 60 and d) 65°C. Scale bars: 200 nm

The resulting particles have for all the syntheses a well ordered hexagonal structure and a well-defined particle morphology. A synthesis temperature of 60 and 65°C give rise to particles with a spherical and a elongated particle morphology, respectively (fig. 5.1c, d). In the two lower temperature cases, a peculiar morphology was obtained (Fig. 5.1a, b). The crystal habit is that of a hexagonal prism, but wedges are missing for a perfect shape. Holes and less dense areas are also identified in the structure for the 50°C synthesis. The small variations in synthesis temperature was shown to have a large impact on the partice morphology and particle size, but only minor changes on the lattice spacing of the well-ordered hexagonal phase. The unusual morphology found in the 50 and 55°C syntheses indicated an extra step in the formation of platelike particles[6], which made the system interesting to explore in more detail. It was concluded that the particles in the 50 and 55°C syntheses were made up of seven smaller particles (primary particles). Primary particles are first formed in the synthseses. These particles aggregate in an oriented way to form a secondary particle. The oriented aggregation was hindered by diluting (1:1) the syntheses at a specific time and hence primary particles were obtained (Fig. 5.2). This specific time is after the floc formation but before the oriented aggregation step.
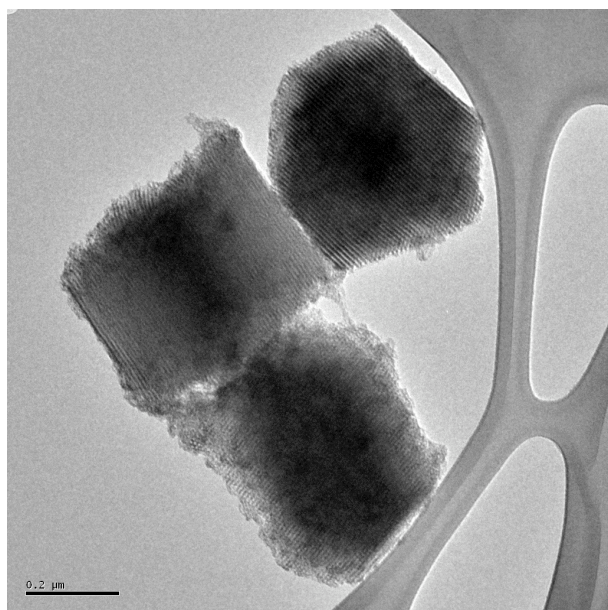

Figure 5.2. TEM image of primary particles synthesesied at 55°C. Scalebar: 200nm

The particles, both primary and secondary, were monodisperse in size and highly ordered. The evolution of the material was followed with time resolved in-situ synchrotron small angle X-ray scattering (SAXS) and ultra small angle X-ray scattering (USAXS) performed at the European syncrotron radiation facility (ESRF) in combination with UV/VIS meaurements[2]. The SAXS region monitor the evolution

of the mesoscopic structure while with USAXS larger objects *i.e.* particles are investigated. Data were collected for syntheses performed at 50, 55, 60 and 65°C. All the syntheses follow the same pattern (except the oriented aggregation step which exclusively occurs at 50 and 55°C). The only difference was the onset and the length of the events. A higher temperature speeds up the formation process. Investigating both the mesoscopic and the colloidal size region is important in order to get a full understanding of the processes taking place in the formation of SBA-15. Figure 5.3 displays a combined USAXS and SAXS diffractogram for 50°C synthesis.
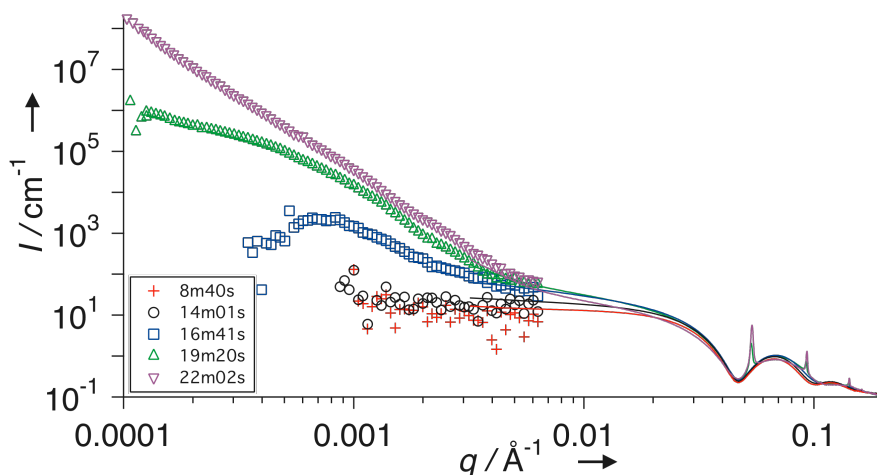

Figure 5.3. Combined in-situ time-resolved SAXS (solid line) and USAXS (dots) data for the 50°C synthesis. Each USAXS curve is recorded over a period of 2min and 45s, while the SAXS curves were recorded in less than a second. The SAXS curve that match in time with the end point of each USAXS run are shown.

Additionally, the evolution of SBA-15 was investigated using small angle neutron scattering (SANS). P104 was used as triblock copolymer and synthesis temperature was set to 50°C. The precursor was varied. TMOS, TEOS and TPOS, was used respectively. In some syntheses, 1M of sodium chloride or sodium bromide was added prior to addition of silica source. The advantage with SANS measurements is the possibility to contrast match (see section 4.1.3). The syntheses were made in three different solvents, H_2O, D_2O and a mixture of the mentioned solvents corresponding to the scattering length density of SiO_2, respectively. The main focus was on the evolution of the (10) Bragg peak. Surprisingly the (10) Bragg peak decreased with time and this behaviour was highly dependent on the solvent. The shrinkage reflects the chemistry in the wall and is explained by the compositional change in the wall during the maturation of the hexagonal order.

A second in-stu time-resolved SAXS study was performed at the Austrian beam line at ELETTRA in Trieste. P104 was used as triblock copolymer and synthesis temperature was set to 45°C The influence of salt on the formation mechanism of

SBA-15 was invetsigated. Different concentrations of sodium chloride, sodium bromide and sodium iodide, respectively, were added to the reaction solution prior to the addition of TEOS. Presence of salt resulted, in all cases, in faster dynamics in the formation of SBA-15.

A model was proposed that explain the morphology of SBA-15 particles based on the relative surface energies of the defining faces of a hexagonol prism. The surface free energy of the interfaces depend on the molecular arrangement. The micelles grow inside the flocs into cylinders. Hence the surface parallel or perpendicular to the direction of the micellar aggregates are different. As a result the surface free energy of the interfaces is different. The synthesis temperature, silica source and presence of NaCl were varied and the obtained morphologies were compared to the presented model. The model describes the observed changes in aspect ratio in height and width of the hexagonal shaped particles (fig. 5.4).
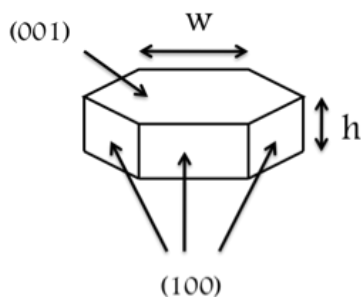

Figure 5.4. A schematic picture of a hexagonal prism, the characteristic morphology for a 2D hexagonal phase. The particle is defined by two (001) faces and 6 (100) faces. The relative surface energies of the faces control the height and width of the particle morphology.

The obtained results in this thesis suggest following steps in the formation of SBA-15.

1. Prior to the addition and just after the addition of the silica precursor the synthesis solution consist of polydisperse spherical P104 micelles. Additon of salt may elongate the micelle sligthly. There is a continous increase in electron density in the palisade layer due to enrichment of siliceous species in the EO-layer. There are no or very small changes in core radius and shell thickness. Figure 5.5 display time resolved SAXS data collected at ESRF. Neither USAXS or UV/VIS monitor any larger structures.
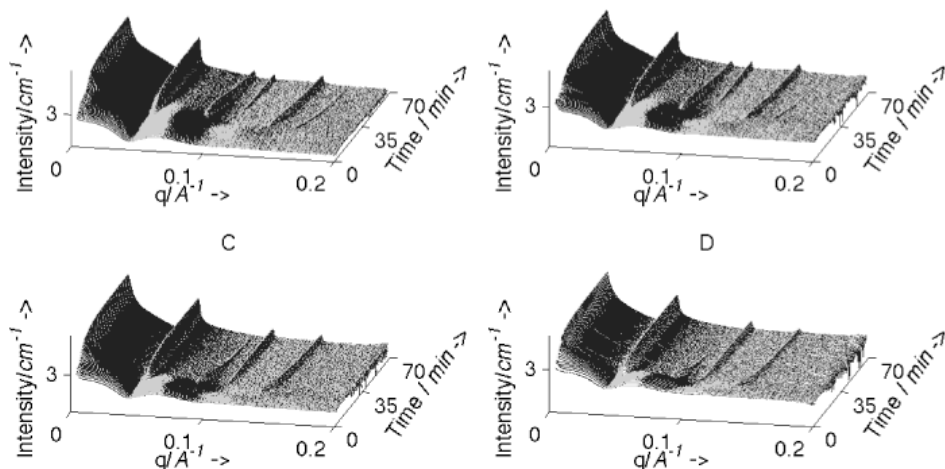
Figure 5.5. Time resolved in situ SAXS data performed at a) 50°C, b) 55°C, c) 60°C and d) 65°C. In all cases, initially the data was fitted to a polydisperse spherical micelle. After some time the SAXS data can not be fitted satisfactorily due to a mixed micellar system. A little bit later the data can be fitted to a polydisperse cylindrical micelle. Eventually, the hexagonal structure appeared. A higher synthesis temperature speeds up the kinetics.

2. Small droplets, flocs, of concentrated pluronic and silica is formed (liquid liquid phase separation) through a nucleation and growth process. The nucleation step is most likely fairly fast. At about the same time as larger objects are identified in the UV/VIS data and shortly thereafter in the USAXS data, the SAXS data cannot be satisfactorily fitted. This is a consequence of a mixed micellar system. The micelles will further grow inside the emulsion drops due to a higher local concentration of surfactant and silica. The curvature of the micelles decreases due to the polymeriszing silica in the palisade layer, which also induces an elongation of the micelles. A higher synthesis temperature or salt additions increases the kinetics and hence the nucleation and growth steps as well as the growth of the cylinders start earlier.

3. The flocs are initially isotropic but become anisotropic due to the elongation of the micelles within the flocs. The floc likely goes through a nematic like phase prior to the hexagonally ordered structure. For a 2D hexagonal liquid crystalline structure one expects the particles to adopt a hexagonal prismatic morphology. In that case, the particle is defined by 2 (001) faces and 6 (100) faces. The equilibrium shape is in general determined by a minimum in the surface free energy of the particle. If the volume of floc is constant and if there is enough flexibility within the particle, the particle will adopt h/w ratio according to

43

$$\frac{h}{w} = \sqrt{3}\,\frac{\gamma_{001}}{\gamma_{100}}$$

(5.1)

γ is the surface tension for the (001) faces and the (100) faces.

4. Depending on synthesis conditions, an oriented aggregation step can occur. In the 50°C and the 55°C syntheses, the transient primary particles aggregate in an oriented way. Seven small particles build up a larger platelike particle. However, a prerequisite for this to happen that is the primary particles have an anisotropic form where the faces have different surface energy. The silica connectivity need to be low and the hexagonal order not fully developed in the liquid like primary particles in order for the aggregation to occur. The aggregation decreases the overall surface free energy of the system. In the 60 and 65°C syntheses this behaviour is not seen. However, oriented aggregation takes place when the synthesis temperature is raised above 65C. However, at this temperature the particles aggregate with the (001) faces (end-to-tail).

5. The hexagonal structure eventually appear. A higher synthesis temperature or an addition of salt induces a faster ordering of the material. Solvent leaves the wall as the silica polymerizes and the structure becomes denser.

6. The particles loosly aggregate in an unspecific manner. The particles partly split up during the filtration and drying of the sample.

7. The silica polymerzation continues long after the hexagonal order and the final particle morphology appeared.

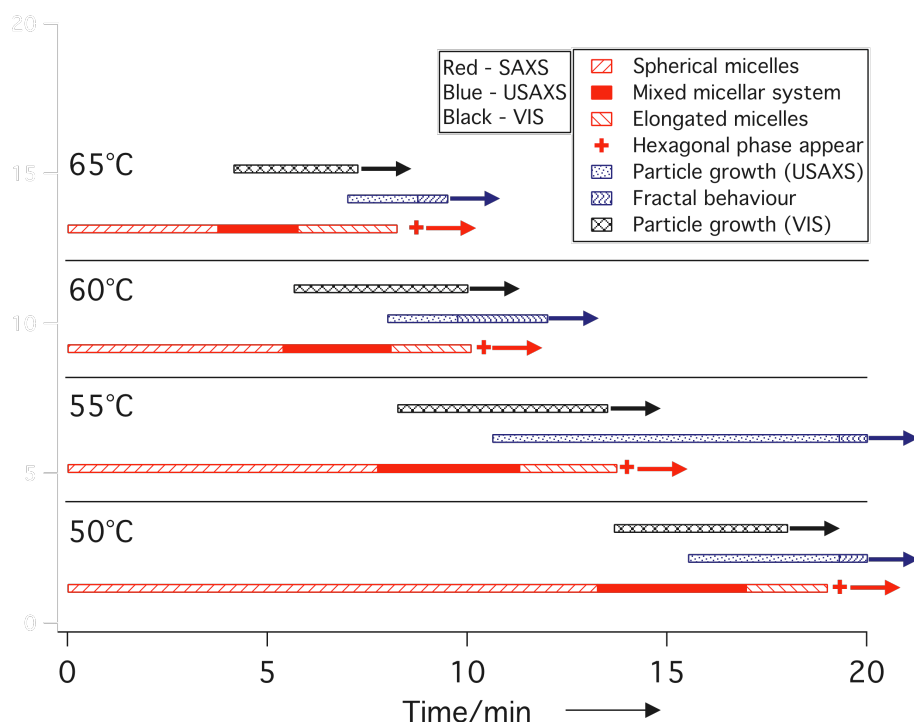Figure 5.6 displays the events taking place for the 50°, 55°, 60° and 65°C synthesis of SBA-15.[2]

Figure 5.6. An overview of the process in the formation of SBA-15 synthesized at 50, 55, 60 and 65°C.

5.2 Tailoring particle morphology (VI)

The knowledge gained from paper 1-5 gave the possibility to control and influence the morphology of the particles. The time resolved synchrotron USAXS combined with UV/VIS study gave information regarding the previosly mentioned steps 1-2 and 4-6 (Fig. 5.6). In the 50° and 55°C syntheses, the growth of the primary particles was finished around 15 and 14 minutes, respectively. The shape of the flocs are most likey anisotropic since the micelles at this stage are no longer strictly spherical. Interestingly, the synthesis solution is, only, a bit more viscous than the micellar solution prior addition of precursor, but transparent, when flocs are present. Therefore, the eye is not a good tool to judge if the solution contains larger structures.

The particle morphology can be controlled at this point by for instance additions of salt or hydrochloric acid. The diameter of the hexagonal prism was varied, while the thickness was kept constant. The arguments used in paper 4 are used to discuss and explain the results. If the synthesis is left unpertub, a "normal" synthesis, it will result in a particle with a diameter of 1.8μm and 1.1μm in the 50 and 55°C syntheses, respectively (Fig. 5.7a and c). We have named them secondary particles or the second

generation of particles (Fig. 1.2). Primary particles or the first generation of particles can be obtained by diluting (1:1) the synthesis solution with 1.6M of hydrochloric acid. The oriented aggregation and the particles have a diameter of 0.6μm and 0.4μm in the 50° and 55°C syntheses, respectively (Fig. 5.7b and d). The size of the primary particles correspond to a primary particle in a secondary particle.
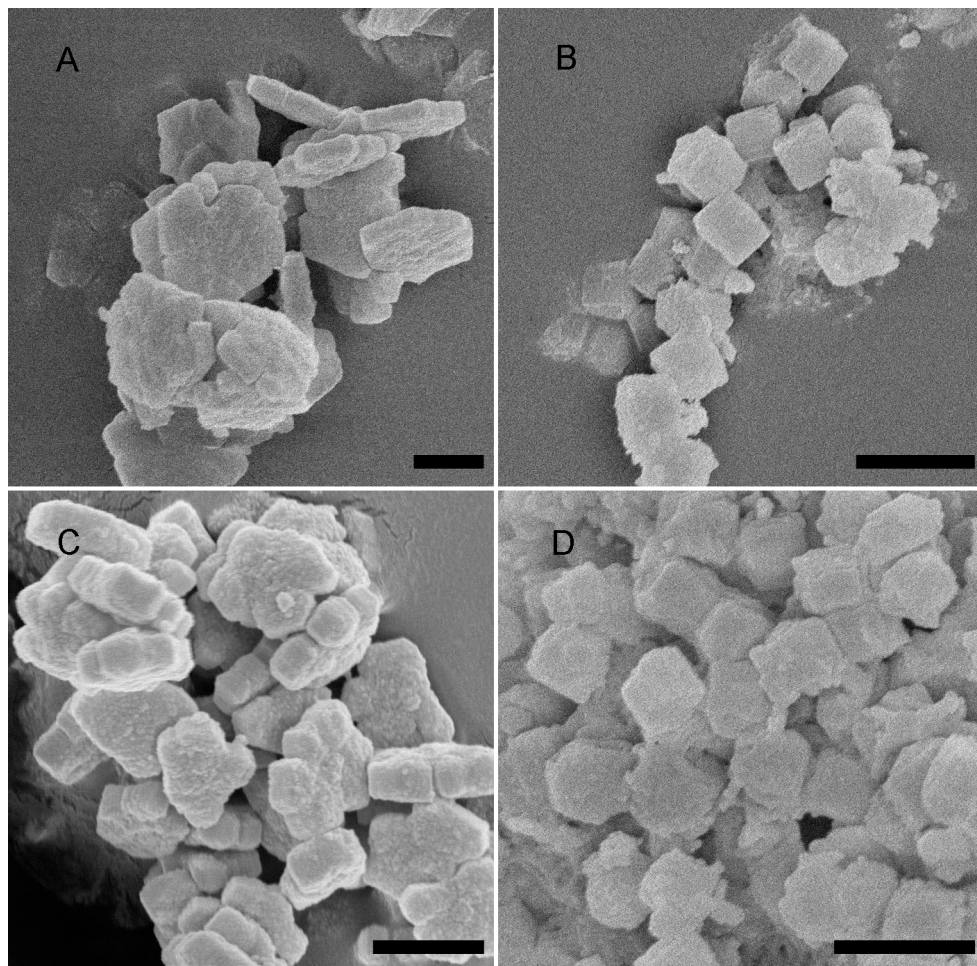

Figure 5.7. SEM images showing secondary and primary particles. Image a) and c) show the particle size and geometry are for a normal 50°C and 55°C synthesis, respectively. A 1:1 dilution of 50°C 1.6 M hydrochloric acid 15 minutes into the reaction and of 55°C 1.6 M hydrochloric acid 14 minutes into the reaction give rise to primary particles (b) and (d), respectively. Scale bars: 1μm.

The oriented aggregation can be enhanced by adding small amounts of salt. The influence of sodium chloride and sodium iodide on the oriented aggregation were

investigated. A small amount of a salt was dissolved in 1.6M of hydrochloric acid, tempered to the synthesis temperature and added to the synthesis mixture at these specific times. The final salt concentration in synthesis mixture was typically 0.01 to 0.5M. A small white precipitate was formed at addition which redissolved. The addition of salt decreased the time of precipitation and increased the diameter of the resulting particles. The increase in diameter was not due to the slight increase in volume or evaporation of solvent during addition. Figure 5.8 show the influence of adding NaI to a 55°C synthesis. The diameter increased and it is possible to see the interfaces between the aggregated primary particles. However, too much salt forces the system to instantly precipitate giving an unspecific aggregation. The resulting particles are in some cases similar to the primary particles in shape and size.
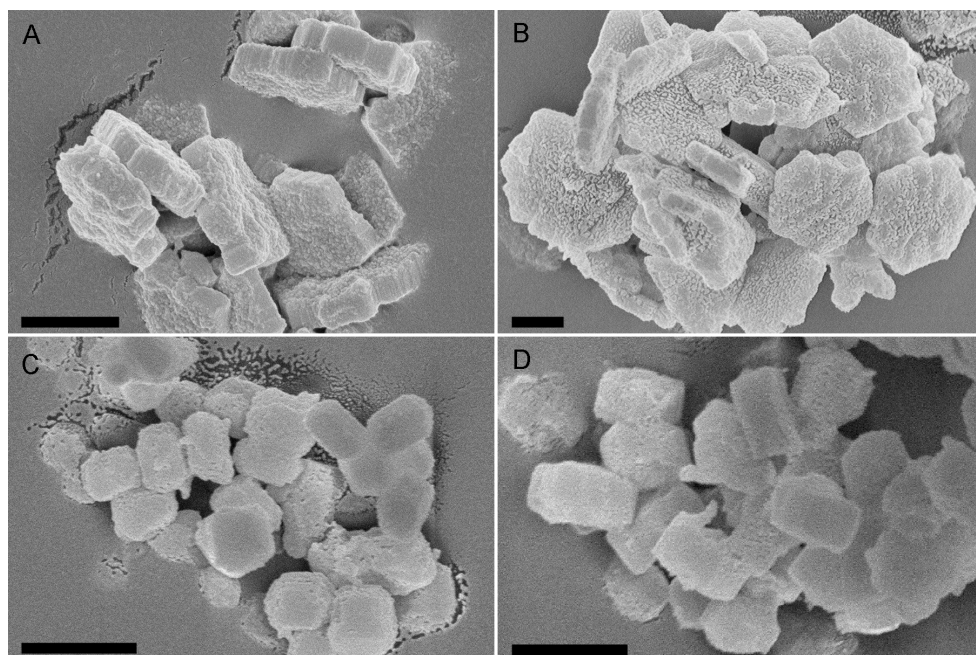

Figure 5.8. The SEM images show the effect of the addition of sodium iodide (a) +0.01 M, (b) +0.02 M, (c) +0.05 M and (d) 0.02 M for the 55°C synthesis. The +sign indicate that sodium iodide was added 14 minutes into the 55°C synthesis and the concentration is the final salt concentration after mixing (a-c), while in the (d) image was sodium iodide prior to addition of TMOS. Scale bars: 1μm.

By adding salt the 3rd and the 4th generation of particles were formed. The concept of generations is schematically presented in figure 1.2.

7. Acknowledgement

Referenser

1   D. Zhao, Q. Huo, J. Feng, B. F. Chmelka and G. D. Stucky, *J. Am. Chem. Soc.*, 1998, 120, 6024-6036.

2   P. Linton, A. R. Rennie, M. Zackrisson and V. Alfredsson, *Langmuir*, 2009, 25, 4685–4691.

3   P. Linton, A. R. Rennie and V. Alfredsson, *Manuscript*.

4   C. V. Teixeira, H. Amenitsch, P. Linton, M. Linden and V. Alfredsson, *Manuscript*.

5   P. Linton, J.-C. Hernandez-Garrido, P. A. Midgley, H. Wennerström and V. Alfredsson, *Phys. Chem. Chem. Phys.*, 2009, DOI: 10.1039/b913755f.

6   P. Linton and V. Alfredsson, *Chemistry of Materials*, 2008, 20, 2878-2880.

7   P. Linton, H. Wennerstroem and V. Alfredsson, *Submitted to Phys. Chem. Chem. Phys.*, 2009.

8   D. F. Evans and H. Wennerström, *The colloidal domain: where physics, chemistry and biology meet.*, Wiley-VCH, New York, Chichester, Weinheim, Brisbane, Singapore, Toronto, 1999.

9   J. Israelachvilli, *Intermolecular and surface forces*, Elsevier, London, 2006.

10   K. Holmberg, B. Jönsson, B. Kronberg and B. Lindman, *Surfactants and polymers in aqueous solution*, John WIley & sons, ltd, Chichester, West Sussex, England, 2004.

11   G. Wanka, H. Hoffmann and W. Ulbricht, *Macromolecules*, 1994, 27, 4145-4159.

12   G. Karlstrom, *J. Phys. Chem.*, 1985, 89, 4962-4964.

13   P. Alexandridis and J. F. Holzwarth, *Langmuir*, 1997, 13, 6074-6082.

14   B. Svensson, P. Alexandridis and U. Olsson, *J. Phys. Chem. B*, 1998, 102, 7541-7548.

15   I. W. Hamley, *Introduction to soft matter*, John Wiley & sons, Chichester, 2004.

16   K. J. Mysels, *Introduction to colloid chemistry*, Interscience publichers, inc., New York, 1967.

17   D. H. Everett, *Basic principles of colloid science*, RSC, Cambridge, 1988.

18   C. T. Kresge, M. E. Leonowicz, W. J. Roth, J. C. Vartuli and J. S. Beck, *Nature*, 1992, 359, 710-712.

19   S. Inagaki, Y. Fukushima and K. Kuroda, *J. Chem. Soc., Chem. Commun.*, 1993, 8, 680-682.

20   J. S. Beck, J. C. Vartuli, W. J. Roth, M. E. Leonowicz, C. T. Kresge, K. D. Schmitt, C. T. W. Chu, D. H. Olson, E. W. Sheppard, S. B. McCullen, J. B. Higgins and J. L. Schlenker, *J. Am. Chem. Soc.*, 1992, 114, 10834-10843.

21   T. Yanagisawa, T. Shimitzu, K. Kuroda and C. Kato, *The chemical society of Japan*, 1990, 988.

22   E. L. Margelefsky, A. Bendjeriou, R. K. Zeidan, V. Dufaud and M. E. Davis, *Journal of the American Chemical Society*, 2008, 130, 13442-13449.

23   M. C. Bruzzoniti, R. M. De Carlo, S. Fiorilli, B. Onida and C. Sarzanini, *Journal of Chromatography, A*, 2009, 1216, 5540-5547.

24   M. Stromme, U. Brohede, R. Atluri and A. E. Garcia-Bennet, *Wiley Interdisciplinary Reviews: Nanomedicine and Nanobiotechnology*, 2009, 1, 140-148.

25   G. S. Attard, J. C. Glyde and C. G. Göltner, *Nature*, 1995, 378, 366-368.

26   C. J. Brinker, Y. Lu, A. Sellinger and H. Fan, *Adv. Mater.*, 1999, 11, 579-585.

27   D. Zhao, J. Feng, Q. Huo, N. Melosh, G. H. Fredrickson, B. F. Chmelka and G. D. Stucky, *Science*, 1998, 279, 548-552.

28   S. Che, A. E. Garcia-Bennet, T. Yokoi, K. Sakamoto, H. Kunieda, O. Terasaki and T. Tatsumi, *Nature Materials*, 2003, 2, 801-805.

29   C. J. Brinker and G. W. Scherer, *Sol-Gel science: the physics and chemistry of sol-gel processing*, Academic press, San Diego, 1990.

30   C. J. Brinker, *Journal of Non-Crystalline Solids*, 1988, 100, 31-50.

31   R. K. Iler, *The chemistry of silica*, A Wiley - Interscience publication, New York, 1979.

32   K. Flodström and V. Alfredsson, *Micropor. Mesopor. Mater.*, 2003, 59, 167-176.

33   P. Kipkemboi, A. Fogden, V. Alfredsson and K. Flodström, *Langmuir*, 2001, 17, 5398-5402.

34   K. Flodström, V. Alfredsson and N. Källrot, *J. Am. Chem. Soc.*, 2003, 125, 4402-4403.

35   F. Kleitz, S. H. Choi and R. Ryoo, *Chemical Communication*, 2003, 2136-2137.

36   F. Kleitz, T.-W. Kim and R. Ryoo, *Langmuir*, 2006, 22, 440-445.

37   B.-C. Chen, H.-P. Lin, M.-C. Chao, C.-Y. Mou and C.-Y. Tang, *Advanced Materials*, 2004, 16, 1657-1661.

38   Sujandi, S.-E. Park, D.-S. Han, S.-C. Han, M.-J. Jin and T. Ohsuna, *Chemical Communication*, 2006, 4131-4133.

39   H. Zhang, J. Sun, D. Ma, X. Bao, A. Klein-Hoffmann, G. Weinberg, D. Su and R. Schlögl, *J. Am. Chem. Soc.*, 2004, 126, 7440-7441.

40   C. Yu, J. Fan, B. Tian and D. Zhao, *Chem Mater*, 2004, 16, 889-898.

41   K. Flodström, C. V. Teixeira, H. Amenitsch, V. Alfredsson and M. Lindén, *Langmuir*, 2004, 20, 4885-4891.

42   K. Flodström, H. Wennerström and V. Alfredsson, *Langmuir*, 2004, 20, 680-688.

43   M. Mesa, L. Sierra and J.-L. Guth, *Microporous and mesoporous materials*, 2008, 112, 338-350.

44   S. Ruthstein, V. Frydman and D. Goldfarb, *J. Phys. Chem. B*, 2004, 108, 9016-9022.

45   S. Ruthstein, V. Frydman, S. Kababya, M. Landau and D. Goldfarb, *J. Phys. Chem. B*, 2003, 107, 1739-1748.

46   S. Ruthstein, J. Schmidt, E. Kesselman, Y. Talmon and D. Goldfarb, *J. Am. Chem. Soc.*, 2006, 128, 3366-3374.

47   A. Y. Khodakov, V. L. Zholobenko, M. Imperor-Clerc and D. Durand, *J. Phys. Chem. B.*, 2005, 109, 22780-22790.

48   M. Impéror-Clerc, I. Grillo, A. Y. Khodakov, D. Durand and V. L. Zholobenko, *Chem. Comm.*, 2007, 834-836.

49   A. Sundblom, C. L. P. Oliveira, A. E. C. Palmqvist and J. S. Pedersen, *The Journal of Physical Chemistry C*, 2009, 113, 7706–7713.

50   D. Zhao, P. Yang, N. Melosh, J. Feng, B. D. Chmelka and G. D. Stucky, *Advanced Materials*, 1998, 10, 1380-1385.

51   F. Hoffmann, M. Cornelius, J. Morell and M. Fröba, *Angew. Chem. Int. ed.*, 2006, 45, 3216-3251.

52   Y. Wan, Y. Shi and D. Zhao, *Chem. Comm.*, 2007, 897-926.

53   P. Lindner and T. Zemb, *Neutrons, X-rays and light. Scattering methods applied to soft condensed matter*, Elsevier Science B.V., Amsterdam, 2002.

54   D. B. Williams and C. B. Carter, *Transmission electron microscopy. Basics I*, Plenum Press, New York, 1996.

55   J. Goldstein, D. E. Newbury, D. C. Joy, C. E. Lyman, P. Echlin, E. Lifshin, L. C. Sawyer and J. R. Michael, *Scanning electron microscopy and X-ray microanalysis*, Plenum Press, New York, 1992.

56   P. A. Midgley, M. Weyland, J. M. Thomas and B. F. G. Johnson, *Chem. Comm.*, 2001, 907-908.

57   P. A. Midgley and M. Weyland, *Ultramicroscopy 96*, 2003, 413-431.